Available online at www.sciencedirect.com

SciVerse ScienceDirect

PHOTONICS AND NANOSTRUCTURES Fundamentals and Applications

Photonics and Nanostructures – Fundamentals and Applications 10 (2012) 547–552

www.elsevier.com/locate/photonics

Ultra-large tuning of photonic modes for efficient Er-doped silicon-based emitters

L. Cavigli [a,*], A. Vinattieri [a], M. Colocci [a], D. Gerace [b], L.C. Andreani [b], A. Piana [c], D. Sanfilippo [c], A. Muscarà [c], E. Marcellino [c], D. Rodilosso [c], M.E. Castagna [c], M. Gurioli [a]

[a] *Dipartimento di Fisica e Astrofisica Università di Firenze, via Sansone 1, 50019 Firenze, Italy*
[b] *Dipartimento di Fisica "A. Volta", Università di Pavia, via Bassi 6, 27100 Pavia, Italy*
[c] *STMicroelectronics, IMS R&D, Stradale Primosole, 50, 95121 Catania, Italy*

Received 29 November 2011; received in revised form 2 April 2012; accepted 25 April 2012
Available online 5 May 2012

Abstract

We demonstrate that a gentle gas adsorption technique can be used to achieve an optimal covering of silicon-based photonic crystal slabs, leading to an unexpectedly large (up to 42 nm) shift of the resonant modes wavelength, with possibility of fine tuning. Strong enhancement (up to 30 times) of the emission band of the Er^{3+} ion into such structures is obtained. Finally, we were able to balance the adsorption and desorption processes by controlling the sample temperature, thus yielding a stable mode at the desired wavelength.

© 2012 Elsevier B.V. All rights reserved.

Keywords: Photonic tuning; Silicon nanostructures; Erbium

1. Introduction

In view of the long lasting goal of integrating all the optical and electronic functions on a single chip, efficient light emission in silicon-based systems and devices is one of the utmost relevant issues in nanophotonics. The combination of silicon (Si) nanostructures and Erbium (Er) doping has been pointed out as very promising due to the enhanced Er^{3+} excitation mediated by carrier capture into the Si nanoclusters [1–3]. Large improvement of the external quantum efficiency has been recently demonstrated by embedding the emitting layers into photonic crystal (PhC) systems, thus tailoring the angular emission and the radiative rate. In particular, a strong enhancement of the external emission efficiency has been obtained in silicon-on-insulator (SOI) PhC slab [4], by the existence of photonic modes at Γ with small group velocity [5–8]

A common problem in fully exploiting the synergy of nanotechnology with photonics is the spectral mismatch between photonic and material resonances. In fact, the coupling efficiency of an emitter to the modes of a PhC structure crucially depends on the ability to deterministically predict the spectral resonance of photonic systems. Unavoidable imperfections arising during the PhC fabrication spectrally detune the

* Corresponding author. Present address: Istituto di Fisica Applicata Consiglio Nazionale delle Ricerche (IFAC-CNR), Via Madonna del Piano 10, 50019 Sesto Fiorentino (FI), Italy.
E-mail addresses: cavigli@fi.infn.it, l.cavigli@ifac.cnr.it (L. Cavigli).

1569-4410/$ – see front matter © 2012 Elsevier B.V. All rights reserved.
http://dx.doi.org/10.1016/j.photonics.2012.04.008

modes from the target wavelength. Postfabrication tuning has been realized with various methods, including digital etching [9], liquid infiltration [10,11], near field perturbation [12,13] and nano-oxidation [14]. One very simple, large (up to 5 nm) and reversible tuning method has been obtained by allowing xenon or nitrogen gas to adsorb onto a PhC slab nanocavity maintained at low temperature [15].

In this work, we demonstrate that the gas adsorption technique can be used to achieve an unexpectedly large shift of the resonant modes wavelength (up to 42 nm), which can be exploited for precise tuning of SOI PhC slab modes, yielding a strong emission enhancement of the Er^{3+} ion into a Si-based structure at the target telecommunication wavelengths around 1.5 μm. Going beyond the approaches reported in previous works, our use of a very slow gas adsorption leads to an optimal covering of the PhC slab with complete infiltration of the air pores. The consequent dielectric perturbation of the PhC modes is optimized to the maximum predicted value, which also depends on the extension of the photonic modes out of the dielectric region. By controlling the sample temperature we are also able to balance the adsorption and desorption processes, thus obtaining a stable mode at the desired wavelength.

The paper is organized as follows. In Section 2 we briefly describe our design, fabrication, and experimental tools; in Section 3 we report our experimental results and comment them, before summarizing the main conclusions of the work in Section 4.

2. Design, fabrication, and experimental methods

Active SOI waveguides were fabricated by depositing a sequence of Si (120 nm, B-doped)/SiO_2:Si-nc:Er (50 nm)/Si (120 nm, As-doped) layers on top of a 1.9 μm thick silicon dioxide layer thermally grown on a Si substrate. Silicon layers have been deposited by Low Pressure Chemical Vapor Deposition (LPCVD), while Silicon Rich Oxide (SRO), characterized by a Si excess of 43%, is grown by Plasma Enhanced Chemical Vapor Deposition (PECVD). Erbium was then introduced in SRO region by ion implantation at energy of 50 keV to a total fluence of 2.5×10^{14} ions/cm^2. The implantation energy has been chosen in order to have the projected range of the ion distribution in the center of the dielectric gate. Subsequently, a thermal annealing was performed on the device at a temperature $T = 800\ ^\circ C$ for 30 min under nitrogen flux, with the goal of achieving the optical activation of Er^{3+} ions and the agglomeration of the Si excess in SRO films to form Si nanocrystals (Si-nc).

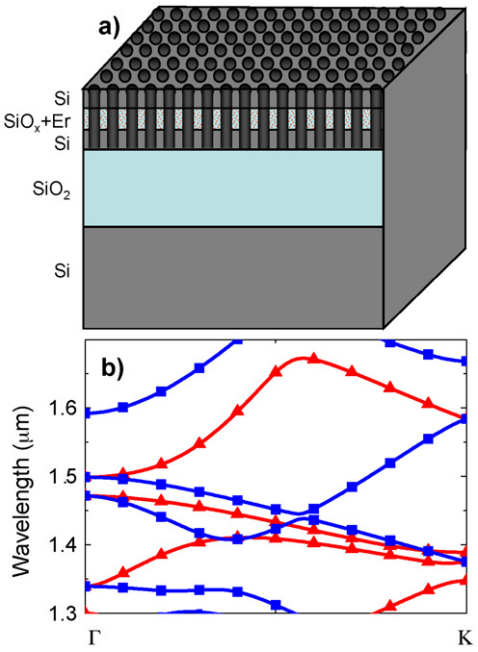

Fig. 1. (a) Scheme of the SOI PhC slab. (b) Photonic band dispersion in the case of $a = 1060$ nm around the wavelength of 1.5 μm; even (odd, respectively) states are plotted in red triangles (blue squares respectively). Around 1.5 μm we see two degenerate states at Γ (even and odd states coincide). (For interpretation of the references to color in this figure legend, the reader is referred to the web version of the article.)

Two-dimensional (2D) PhC were fabricated into the SOI waveguide by means of standard electron beam lithography and reactive ion-etching techniques. The structure under consideration consists of a 2D triangular lattice of air holes; a schematic picture of the PhC is reported in Fig. 1(a). Several samples were fabricated with lattice constants varying from $a = 1000$ nm to $a = 1240$ nm in steps of 20 nm in order to provide the energy matching between the Er^{3+} emission line and a photonic mode around $\boldsymbol{k} = 0$, i.e., at the Γ point of the 2D Brillouin zone. The hole radius to lattice constant ratio, $r/a = 0.33$, was kept constant for all samples.

A guided mode expansion (GME) method [16] has been applied for the structures design. The method is based on calculating the photonic band dispersion in PhC slabs by expanding the modes of the three-layer structure (upper cladding/core/lower cladding) on the basis of guided modes of an effective planar waveguide. A typical calculation is shown in Fig. 1(b) for the PhC slab with lattice constant $a = 1060$ nm, reported for wavelengths around 1.5 μm. For the core layer we used an average refractive index to take into account the composite nature of this layer [4]. Even (odd) modes due to reflection symmetry with respect to the vertical

plane of incidence along the ΓK direction in the first Brillouin zone of the hexagonal lattice are plotted in with red triangles (blue squares). The calculated photonic band diagram of the PhC slab shows the existence of photonic modes λ_{ph} around 1.5 μm that are degenerated at Γ and split into modes of opposite parities, which will be discussed in the following.

Photoluminescence (PL) and reflectance (R) spectra at normal incidence were measured in the same point of the sample. The PL was excited by a cw frequency doubled Nd:YAG (yttrium aluminum garnet) laser (532 nm) with a power of 1 mW focused to a spot of 20 μm on the sample surface. Reflectance or PL signals from the sample were collected by a low numerical aperture (NA) objective, sent into a spectrometer and the exiting light was detected by a cooled InGaAs array. The sample was set in a cold finger cryostat in order to change the temperature from 20 K up to room temperature.

3. Results and discussion

Typical reflectivity and PL spectra at room temperature are reported in Fig. 2 for three different structures (a = 1000 nm, a = 1040 nm, a = 1080 nm). In the same figure, we also report for sake of comparison the PL spectrum from a sample without the PhC pattern, showing the emission band from the active SiO_2:Si-nc:Er layer. Note that the Er^{3+} emission band is strongly enhanced (nearly 20 times) by the presence of the photonic mode, with respect to the sample without the PhC. Reflectance spectra show two main dips associated to the photonic resonances of the SOI slab at normal incidence (see also Fig. 1b). These modes have been exploited in Ref. [4] for enhancing the Er^{3+} emission band, as due to the increase in the photonic density of states also related to the small group velocity [5–8]. The reflectance dips have Q factors of the order of 100, which is a good compromise for achieving high enhancement over a quite broad spectral range, with the goal of increasing the extraction efficiency across most of the Er^{3+} emission band. Therefore we observe an overall enhancement of the Er^{3+} emission, even when the energy of the photonics resonances does not match exactly with the maximum of the Er^{3+} emission band (as for example for the sample with a = 1080 nm, green line and squares in Fig. 2). Otherwise, when the photonic modes is resonant with the Er^{3+} emission band (a = 1000 nm, black lines and full circles in Fig. 2) the PL intensity is maximum and no distortion in the spectra is observed, as we compare with PL spectrum in the sample without PhC pattern (inset of Fig. 2). In the intermediate cases, selective enhancements of the different contributions can be clearly observed, with a slight distortion of the Er^{3+} emission band. The emission is enhanced only for those energies which are in resonance with a photonic mode; they correspond closely to the peak positions in PL and to the resonant structures in R spectra (a = 1040 nm, red lines and triangles in Fig. 2). The comparison between calculated frequencies of the photonic resonances (Fig. 1b) and experimental results is very satisfactory and it clearly demonstrates that the observed enhancement of emission is indeed due to coupling of Er^{3+} emission to the photonic modes of the PhC slab at $\Gamma = 0$, giving an increasing of light extraction efficiency from the device in the vertical direction [4]. By comparing the different reflectance spectra we see that the tuning step $\Delta\lambda = \lambda_{ph} - \lambda_{Er}$ of the PhC mode (λ_{Er} = 1.53 μm corresponding to Er^{3+} emission line), related to the variation of the lattice constant a of 20 nm, is of the order of $\Delta\lambda$ = 15–20 nm, which is too large for a fine control of the coupling with the Er^{3+} emission line. Therefore a precise, but also quite large (i.e. 20 nm), post fabrication tuning process is needed to achieve a full control of the Er^{3+} emission process.

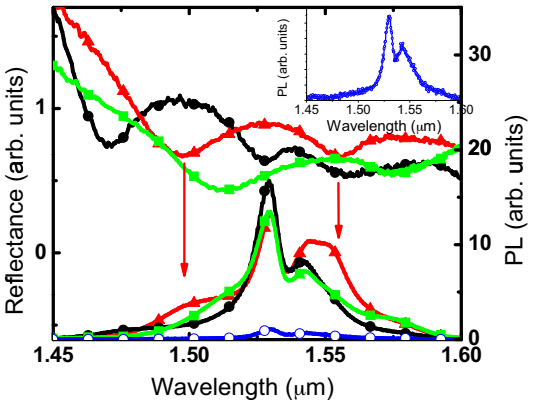

Fig. 2. Comparison between reflectance and PL spectra for three samples with different lattice constant: black line and full circles a = 1000 nm, red line and triangles a = 1040 nm, green line and squares a = 1080 nm. In addition the PL of the sample without PhC is reported as the blue line with open circles in the same graph and in the inset. (For interpretation of the references to color in this figure legend, the reader is referred to the web version of the article.)

We intend to exploit the gas adsorption techniques introduced in Ref. [15] for controlling the strong coupling between a single quantum dot and the mode of a L3 PhC microcavity (MC) on a GaAs membrane; the photonic mode was at 1.2 μm. In Ref. [15] a large amount of gas (Xe or N_2 at 0.5 Torr in a 0.75 l volume) was introduced in the cryostat (where the sample was

set at $T = 4$ K) for each cycle and the gas adsorption time was approximately 1 min. The shift of the cavity peak was almost simultaneous with the gas adsorption and, after recovery of the initial pressure, the cycle was repeated. In the case of Xe (N_2) the shift of the cavity peak saturated at a value of 5 (4) nm after a sequence of the order of 30 cycles. We numerically simulated the experiment of Ref. [15] for evaluating the actual coverage obtained by this gas adsorption technique. Extrapolating from existing data [17] a value of 1.47 for the refractive index of the solid Xe at the wavelength of 1.2 μm and $T = 4$ K, we found that with the complete filling of all the air pores of the PhC and with 100 nm overlayers (above and below the slab) the predicted shift should be as large as 50 nm. This result shows that the gas adsorption procedure used in Ref. [15] was not producing a uniform coverage, possibly due to a rather fast gas adsorption that might lead to clustering of the adsorbed gas on the surface.

Following this analysis, we decided to implement a different processing protocol based on a very slow gas adsorption. In particular we kept the sample at low temperature and at an overpressure of 10^{-5} mbar by continuously pumping in presence of very small air leakage (that is in the very common experimental condition) leading to a slow adsorption of air (that is mainly N_2) on the sample. In Fig. 3 we report the experimental spectra at different times from top to bottom. The time step between two adjacent spectra was of the order of 2 h. We found that the PhC modes are slowly and continuously shifted towards the red, as shown in Fig. 3. The difference with previous results is striking. To better appreciate the result, we report in Fig. 4 the PhC reflectance dips wavelength as a function of the deposition time. The dashed line is a fit based on an exponential growth with a constant rise-time of 5 h. After 10–15 h the shift saturates at a value of the order of 42 nm, which is 1 order of magnitude larger than the values reported in the case of the PhC MC [15]. By choosing a PhC with a mode blue shifted by 20 nm with respect to the Er^{3+} resonance we obtained a very fine tuning across the whole Er^{3+} emission band, which results in a strong enhancement of the light emission from a Si-based structure. Enhancements of the spectrally integrated PL up to 30 times, with respect to the structures without PhC waveguide, were typically found at the optimal tuning, as shown in the inset of Fig. 4.

In order to confirm that the slow deposition is a key ingredient for obtaining a large mode shift, we performed additional measurements (see Fig. 5). We started the gentle gas deposition at the pressure of 10^{-5} mbar for 200 min obtaining a total shift of 19 nm, that is almost half of the total shift observed in Fig. 4 after 1200 min. Then we introduced in the chamber a pressure of 10^{-3} mbar, we waited for 30 min to allow deposition observing a shift of only 1 nm. We repeated the procedure with a pressure of 4 mbar in the chamber

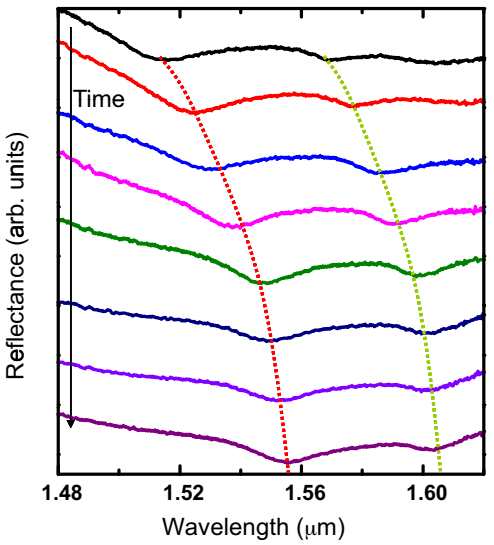

Fig. 3. Series of reflectance spectra taken at different times (from top to bottom with steps of the order of 2 h) of gas adsorption for the sample with lattice constant $a = 1060$ nm, corresponding to a mismatch of 20 nm at the blue side with respect to Er^{3+} resonance. Dotted lines are guides for the eyes. (For interpretation of the references to color in this figure legend, the reader is referred to the web version of the article.)

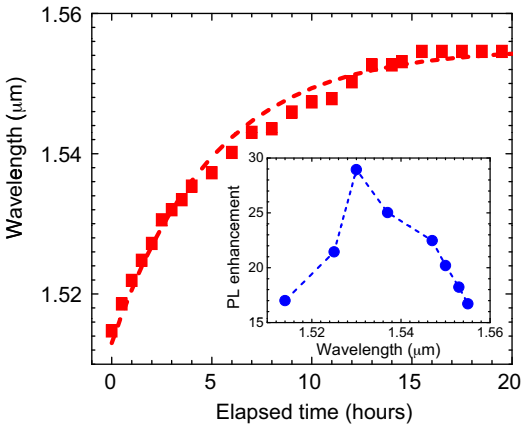

Fig. 4. Spectral position of the PhC mode as a function of the elapsed time after the beginning of gas adsorption. The dashed line is a fit, based on an exponential rise with a time constant of 5 h. In the inset: values of the spectrally integrated PL of the Er^{3+} emission band, normalized to the same quantity as measured in the sample without the PhC fabrication. Data are reported as a function of the dips position in reflectance spectra.

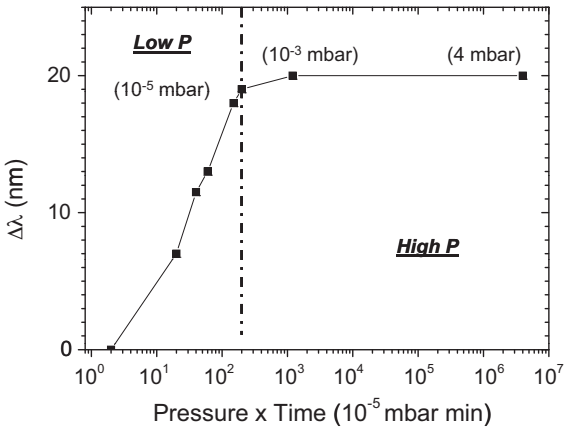

Fig. 5. Trend of the tuning step $\Delta\lambda$ at 22 K as a function of time and different N_2 pressures.

and after 30 min no additional shift was observed. A summary of the data is reported in Fig. 5.

We simulated this process by GME calculations [16], assuming gas adsorption with complete filling of the PhC air pores and with an overlayer cladding deposition; whose results are shown in Fig. 6. Several interesting features are worth being remarked. (i) The shift is different for the two modes, denoting a different spatial distribution of the modes. Obviously, the mode with a wider extension in the air region is more sensitive to the adsorption. (ii) For an index of refraction of 1.47 we have a very large shift, up to 150 nm for the mode at lower wavelength, which is three times larger than the maximum theoretical shift in MC (see discussion above). (iii) The experimental shift of 42 nm is obtained with an index of refraction of the order of 1.2, which nicely agrees with the value reported for liquid and solid nitrogen in the literature [18,19], which can be reasonably assumed to be consistent with the one of the adsorbed air on the slab.

The gas adsorption is obviously a reversible process. By heating the sample above 90 K the original spectral resonance was recovered in a few minutes, due to gas desorption. Then the experiment can be repeated without any degradation of the sample. In order to have a stable device with the optimal spectral matching we exploited the temperature control to balance the gas adsorption and gas desorption processes. In Fig. 7 we report the data from the sample with a native blue detuning of the order of 20 nm; we started by cooling at 22 K the sample and we waited until the air adsorption produced a PhC mode shift up to match the Er^{3+} resonance (the adsorption shift was monitored live). Afterwards we switched on the heater for quickly raising the sample temperature to the different target values (reported in Fig. 7). For $T < 55$ K the gas adsorption dominates and a saturation value of the PhC mode shift is eventually reached after some time. For $T > 55$ K, on the contrary, the gas desorption dominates and the PhC resonance shifts back to the original value of a negative detuning of -20 nm. At $T = 55$ K a balance between the two processes is reached and the PhC mode wavelength remains constant with time.

We therefore demonstrated that the tuning range can be as large as 40 nm, with a sensitivity limited only by the quality of the cryostat vacuum. In the present case we have an averaged tuning rate slower than of 0.1 nm

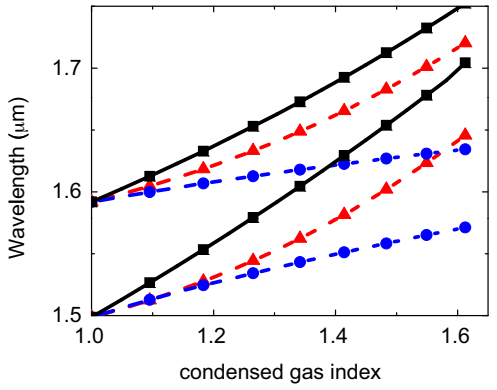

Fig. 6. Results of the simulations for the wavelengths of the two degenerate modes at Γ for different values of the refraction index of the adsorbed gas. Blue lines with dots refer to infiltration of the air pores, red lines with triangles refer to a clad deposition of 100 nm, black lines with squares is the total effect. (For interpretation of the references to color in this figure legend, the reader is referred to the web version of the article.)

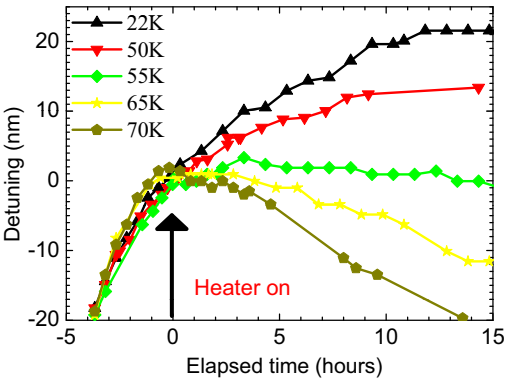

Fig. 7. Spectral detuning of the PhC mode with respect to Er^{3+} resonance as a function of the time elapsed after the beginning of the gas adsorption. Time equal to zero corresponds to the instant at which the resonance matching is achieved and the temperature was raised. Negative times refer to the initial stage when $T = 22$ K and the air adsorption is very effective. Positive times refer to higher value of T as reported by different symbols.

per minute, thus leading to a possible accuracy better than few 0.01 nm. The photonic mode can be stabilized at the desired wavelength for long operation time simply by controlling the temperature at $T = 55$ K. Qualitatively similar, but numerically different, results may be obtained by choosing different adsorption gas

4. Conclusions

In conclusion we have reported on the realization of a stable and optimized light-matter interaction in a silicon based PhC slab light emitter. The novelty is the use of a slow and gentle gas adsorption, which allows an optimal covering of the PhC slab with a complete filling of the PhC air pores. The dielectric perturbation produces a slow tuning and results in a large (up to 42 nm) red shift of the PhC modes. By controlling the temperature we were also able to balance the adsorption and desorption processes and obtaining, in this way, a stable mode at the desired wavelength. The results may be relevant for applications requiring a precise tuning and stabilization of cavity modes, like quantum-electrodynamical experiments employing with PhC cavities

Acknowledgment

We acknowledge financial support from MIUR through FAR 851 project.

References

[1] M. Fujii, M. Yoshida, Y. Kanzawa, S. Hayashi, K. Yamamoto, Applied Physics Letters 71 (1997) 1198.
[2] H.-S. Han, S.-Y. Seo, J.H. Shin, Applied Physics Letters 79 (2001) 4568.
[3] F. Iacona, D. Pacifici, A. Irrera, M. Miritello, G. Franzò, F. Priolo, D. Sanfilippo, G. Di Stefano, P.G. Fallica, Applied Physics Letters 81 (2002) 3242.
[4] M. Galli, A. Politi, M. Belotti, D. Gerace, M. Liscidini, M. Patrini, L.C. Andreani, M. Miritello, A. Irrera, F. Priolo, Y. Chen, Applied Physics Letters 88 (2006) 251114.
[5] E. Viasnoff-Schwoob, C. Weisbuch, H. Benisty, S. Olivier, S. Varoutsis, I. Robert-Philip, R. Houdré, C.J.M. Smith, Physical Review Letters 95 (2005) 183901.
[6] V.S.C. Manga Rao, S. Hughes, Physical Review B 75 (2007) 205437.
[7] G. Lecamp, P. Lalanne, J.P. Hugonin, Physical Review Letters 99 (2007) 023902.
[8] T. Lund-Hansen, S. Stobbe, B. Julsgaard, H. Thyrrestrup, T. Sünner, M. Kamp, A. Forchel, P. Lodahl, Physical Review Letters 101 (2008) 113903, Physical Review B 75 (2007) 205437.
[9] K. Hennessy, A. Badolato, A. Tamboli, P.M. Petroff, E. Hu, M. Atatüre, J. Dreiser, A. Imamoglu, Applied Physics Letters 87 (2005) 021108.
[10] S.W. Leonard, J.P. Mondia, H.M. van Driel, O. Toader, S. John, K. Busch, A. Birner, U. Gösele, V. Lehmann, Physical Review B 61 (2000) R2389.
[11] S. Vignolini, F. Intonti, M. Zani, F. Riboli, D.S. Wiersma, L.H. Li, L. Balet, M. Francardi, A. Gerardino, A. Fiore, M. Gurioli, Applied Physics Letters 94 (2009) 151103.
[12] F. Intonti, S. Vignolini, F. Riboli, A. Vinattieri, D.S. Wiersma, M. Colocci, L. Balet, C. Monat, C. Zinoni, L.H. Li, R. Houdré, M. Francardi, A. Gerardino, A. Fiore, M. Gurioli, Physical Review B 78 (2008) R041401.
[13] S. Vignolini, F. Intonti, L. Balet, M. Zani, F. Riboli, A. Vinattieri, D.S. Wiersma, M. Colocci, L. Li, M. Francardi, A. Gerardino, A. Fiore, M. Gurioli, Applied Physics Letters 93 (2008) 023124.
[14] K. Hennessy, C. Högerle, E. Hu, A. Badolato, A. Imamoglu, Applied Physics Letters 89 (2006) 041118.
[15] S. Mosor, J. Hendrickson, B.C. Richards, J. Sweet, G. Khitrova, H.M. Gibbs, T. Yoshie, A. Scherer, O.B. Shchekin, D.G. Deppe, Applied Physics Letters 87 (2005) 141105.
[16] L.C. Andreani, D. Gerace, Physical Review B 73 (2006) 235114.
[17] A.C. Sinnock, Journal of Physics. C: Solid State Physics 13 (1980) 2375.
[18] D.R. Lide, Handbook of Chemistry and Physics, 82nd ed., CRC, 2001, pp. 4–147.
[19] H.E. Hallam, G.F. Scrimshaw, in: H.E. Hallam (Ed.), Vibrational Spectroscopy of Trapped Species, Wiley, London, 1973.